

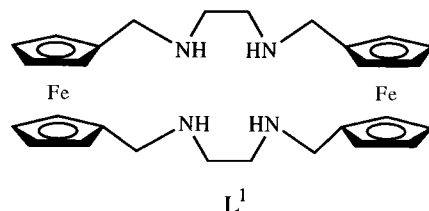
**Electrochemical Sensing of Mercury over Cadmium and Lead Cations
by the Redox-Active Polyazacycloalkane Ligand
1,1':1',1'''-Bis[ethane-1,2-diylbis(iminomethylene)]bis[ferrocene]**

by José M. Lloris, Angel Benito, Ramón Martínez-Máñez,* Miguel E. Padilla-Tosta, Teresa Pardo, Juan Soto,
and María José L. Tintero

Departamento de Química, Universidad Politécnica de Valencia, Camino de Vera s/n, E-46071 Valencia

The coordination behaviour of the redox-active polyazacycloalkane L^1 against the toxic heavy-metal ions Cd^{2+} , Pb^{2+} , and Hg^{2+} was studied in THF/ H_2O 70:30 (containing $0.1 \text{ mol} \cdot \text{dm}^{-3}$ of $(Bu_4N)ClO_4$). The crystal and molecular structure of the cadmium complex $[Cd(L^1)(NO_3)_2]$ (**1**) was determined by X-ray single-crystal analysis. The cadmium ion is in a 4+2 surrounding with the ligand L^1 acting as tetradentate and the apical positions occupied by the O-atoms of the nitrate anions. An electrochemical study reveals that L^1 shows a selective electrochemical response against Hg^{2+} over Cd^{2+} and Pb^{2+} .

Introduction. – There is a considerable interest in the synthesis of compounds bearing both electro-active moieties and binding domains as new ligands for the electrochemical sensing of substrates. Thus, different redox units have been covalently attached to a large variety of binding domains for the sensing of alkaline, earth-alkaline [1], transition-metal ions [2], anions [3], and neutral molecules [4]. We have recently synthesized ferrocene-containing polyazacycloalkane ligands and have observed that their electrochemical response in the presence of transition-metal ions can be modulated as a function of the proton concentration in solution [5]. Additionally, we have prepared new redox-active ligands specifically designed to display electrochemical response towards ions of special interest in environmental chemistry and have reported that ferrocene-functionalized aza-oxa-crown derivatives can electrochemically and selectively detect mercury over other cations commonly present in water [6]. We report here a more detailed study of the electrochemical response of the ligand L^1 against toxic heavy metal ions such as Cd^{2+} , Pb^{2+} , and Hg^{2+} . The molecular structure of complex $[Cd(L^1)(NO_3)_2]$ (**1**) is also reported.



Experimental. – *General.* The ligand 1,1':1',1'''-bis[ethane-1,2-diylbis(iminomethylene)]bis[ferrocene] (L^1) was synthesized following [7]. Tetrahydrofuran (THF) was freshly distilled from sodium benzophenone and used for THF/ H_2O 70:30 (v/v) which was employed in the electrochemical studies. $(Bu_4N)ClO_4$ ($0.1 \text{ mol} \cdot \text{dm}^{-3}$) was used as supporting electrolyte in this solvent mixture.

[1,1'':1',1'''-Bis[ethane-1,2-diylbis[(imino-κN)-methylene]]bis[ferrocene]]bis[nitrato-κO]cadmium (**1**). A mixture of L¹ (100 mg, 0.18 mmol) and stoichiometric amounts of Cd(NO₃)₂·4H₂O (55 mg, 0.18 mmol) was refluxed in MeOH for 3 h. The resulting soln. was evaporated and the yellow powder recrystallized by slow diffusion of Et₂O into a soln. of the solid in CH₂Cl₂: 107 mg (76%) of **1**. IR (KBr): 3422s, 2949w, 1618m, 1500w, 1468m, 1231m, 1102w, 1038w, 841s, 732w. Anal. calc. for C₂₈H₃₆CdFe₂N₆O₆: C 51.20, H 5.50, N 12.80; found: C 51.2, H 5.45, N 12.80.

Physical Measurements. Cyclic voltammograms were obtained with a programmable function generator Tacussel IMT-1, connected to a Tacussel-PJT-120-1 potentiostat. The working electrode was Pt with a sat. calomel reference electrode separated from the test soln. by a salt bridge containing the solvent/supporting electrolyte. The auxiliary electrode was Pt-wire. Potentiometric titrations were carried out under N₂ in THF/H₂O 70:30 using a water-thermostatted vessel (25.0 ± 0.1°). The titrant was added by a Crison microburette 2031. The potentiometric measurements were made using a Crison-2002 pH meter and a combined glass electrode. The titration system was automatically controlled by a personal computer using a program that monitored the *e.m.f.* values and the volume of titrant added. The electrode was calibrated as a H⁺-concentration probe by titration of well-known amounts of HCl with CO₂-free KOH soln. and determination of the equivalent point by *Gran's* method [8] which gives the standard potential *E*⁰ and the ionic product of water (*K*_w = [H⁺][OH⁻]). The concentration of the lead(II), mercury(II), and cadmium(II) solns. were determined using standard methods. The computer program SUPERQUAD [9] was used to calculate the protonation and stability constants.

*Structure Determination of 1*¹). *Crystal Data.* C₂₈H₃₆CdFe₂N₆O₆, *M* 656.63, monoclinic, space group *C2/c*, *a* = 13.727(5), *b* = 15.124(5), *c* = 14.731(6) Å, β = 107.72(3)°, *V* = 2913(2), Å³, *Z* = 4, *D*_c = 1.497 g cm⁻³, λ(MoK_α) = 0.71069 Å, crystal size 0.25 × 0.22 × 0.12 mm, μ = 17.4 cm⁻¹.

Data Collection and Refinement. A well-shaped yellow crystal was mounted on a Siemens-P4 four-circle diffractometer. Unit-cell dimensions were determined from the angular setting of 25 reflections. A monoclinic cell was obtained, and the space group *C2/c* was confirmed from the structure determination. A total of 1996 reflections were collected of which 1904 were unique (4.12 ≤ 2θ ≤ 45.0°) using the 2θ – ω method. The intensity of three standard reflections monitored every 60 min showed no systematic variation. *Lorentz*, polarization, and absorption (*ψ* scan) corrections were applied. The structure was solved by direct methods and refined by full-matrix least-squares on *F*² (SHELXTL) [10]. The cyclopentadienyl groups around Fe(1) and the NO₃⁻ anions were modelled as disordered, bearing in mind that during the refinement, some atoms modelled highly anisotropically and some meaningless C(Cp)–C(Cp) and N–O bond distances were found. The final refinement converged at *R*₁ 0.052 (*F* > 4σ(*F*), for 1084 reflections) and *R*₂ 0.173 (all data). The largest peak and hole in the final difference map were +0.77 and –0.51 eÅ⁻³, respectively.

Results and Discussion. – *Crystal Structure of [Cd(L¹)(NO₃)₂]. (1).* The crystal structure of the cadmium complex **1** of L¹ consists of discrete neutral [Cd(L¹)(NO₃)₂] units linked by *van der Waals* interactions. *Fig. 1,a*, displays a view of the molecule showing the atomic numbering scheme, and in *Tables 1* and *2*, the non-H atomic coordinates and selected bond distances and angles, respectively, are given¹). The Cd-atom is in a 4 + 2 surrounding with the L¹ ligand acting as tetradentate. The 4 N-atoms and the 2 O-atoms around the Cd-atom define a distorted octahedral coordination polyhedron. The equatorial plane is defined by 4 N-atoms (N(1), N(2), N(1)ⁱ, and N(2)ⁱ) belonging to the L¹ receptor, while the apical positions are occupied by 2 O-atoms (O(1) and O(1)ⁱ) of two nitrate anions. The Cd–N bond distances Cd(1)–N(1) (2.308(8) Å) and Cd(1)–N(2) (2.336(10) Å) are shorter than those involving the nitrate ligand (2.50(4) Å for Cd(1)–O(1) and Cd(1)–O(4)). The Fe(1), Cd, and Fe(2) atoms lie on a twofold rotation axis which relates half of the molecule with the

¹) Crystallographic data (excluding structure factors) for the structure reported in this paper have been deposited with the *Crystallographic Data Centre* as deposition No. CCDC-101450. Copies of the data can be obtained, free of charge, on application to the CCDC, 12 Union Road, Cambridge CB2 1EZ, UK (fax: +44(1223)336033; e-mail: deposit@ccdc.cam.ac.uk).

other half. Intramolecular Fe–Cd distances are not equal, Cd–Fe(1) being shorter (Cd–Fe(1) 4.114 and Cd–Fe(2) 5.303 Å). Noticeable disorder was found and modelled during the refinement of the structure around one ferrocenyl group and the nitrate anions. *Fig. 1,b*, gives an alternative view of molecule **1** showing the final atoms found in the disordered part of the molecule. The smaller bond angle around the Cd-atom is in the five members ring N(1)–Cd–N(2) (78.8(4)°) related to the coordinated ethylenediamine moiety which adopts the usual half-chair conformation (torsion angle N(2)–C(3)–C(2)–N(1) 67.9°). Fe–Cp distances range from 1.620 to 1.668 Å with an average distance of 1.654 Å, Fe–C(Cp) bond lengths from 1.91(6) to

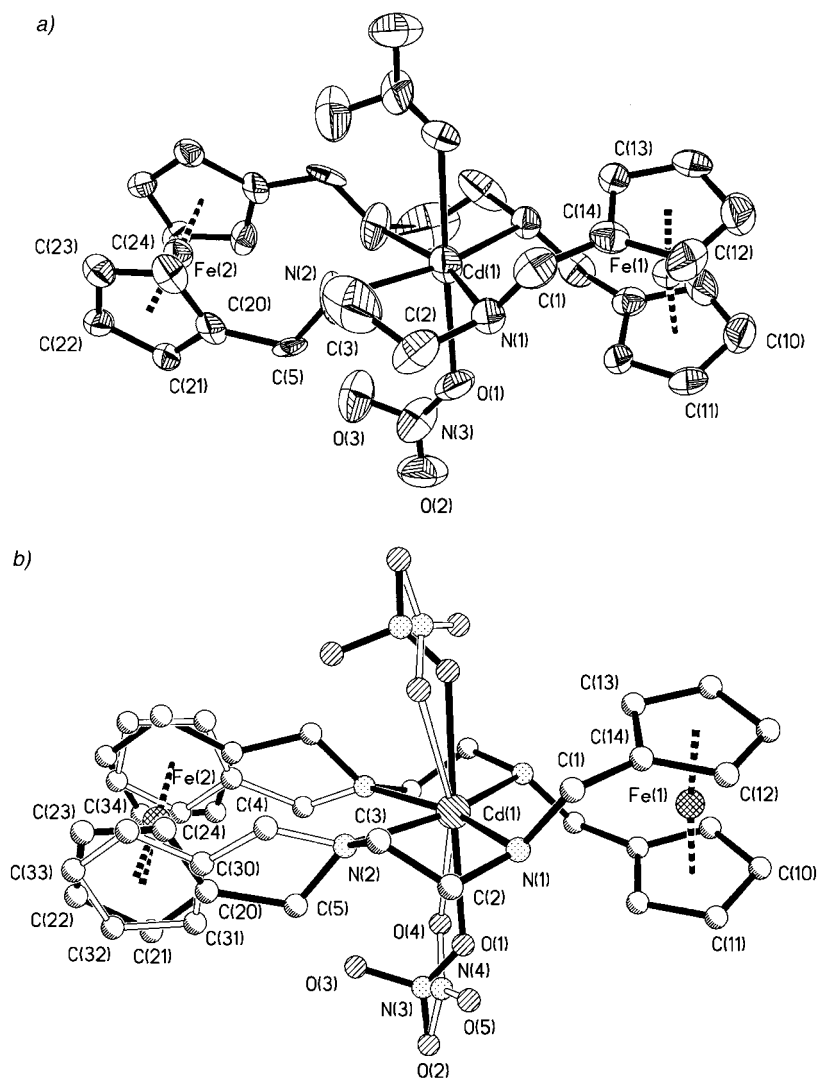


Fig. 1. Crystal structure of $[Cd(L^1)(NO_3)_2]$ (**1**) showing the atomic numbering scheme

Table 1. Atomic Coordinates ($\times 10^4$) and Equivalent Isotropic Displacement Parameters (in $\text{\AA}^2 \times 10^3$) for $[\text{Cd}(\text{L}^1)(\text{NO}_3)_2]$ (1). $U(\text{eq})$ is defined as one third of the trace of the orthogonalized U_{ij} tensor.

Atom	<i>x</i>	<i>y</i>	<i>z</i>	<i>U</i> (eq)
Cd(1)	5000	5752(1)	7500	67(1)
Fe(1)	5000	3031(2)	7500	51(1)
Fe(2)	5000	9258(2)	7500	50(1)
N(1)	6243(7)	4972(6)	8625(6)	52(2)
N(2)	5979(9)	6901(7)	8384(9)	84(4)
N(3)	3677(35)	6233(43)	9014(46)	83(15)
O(1)	3962(41)	5724(24)	8630(31)	110(16)
O(2)	3205(10)	6204(8)	9518(8)	114(4)
O(3)	3797(20)	7033(16)	8793(20)	111(10)
C(1)	6924(9)	4362(8)	8323(9)	71(4)
C(2)	6820(11)	5675(10)	9308(8)	98(6)
C(3)	7005(13)	6416(13)	8868(14)	152(9)
C(5)	5545(15)	7511(16)	8849(10)	51(7)
C(10)	4000(12)	2197(9)	7801(12)	82(5)
C(11)	4412(11)	2768(9)	8584(10)	71(4)
C(12)	6511(10)	2716(8)	7985(11)	74(4)
C(13)	5836(9)	3651(8)	6738(8)	54(3)
C(14)	6397(8)	3608(8)	7701(8)	54(3)
C(20)	5689(39)	8501(35)	8721(26)	52(10)
C(21)	5069(26)	9265(30)	8876(23)	53(8)
C(22)	5547(33)	10047(27)	8658(31)	54(9)
C(23)	6408(29)	9780(26)	8349(24)	56(8)
C(24)	6475(32)	8841(26)	8380(26)	59(9)
C(4)	6415(22)	7724(15)	8374(20)	71(11)
C(30)	5855(53)	8531(46)	8477(43)	60(12)
C(31)	5129(33)	8741(33)	8822(27)	56(9)
C(32)	5174(37)	9698(33)	8870(30)	47(9)
C(33)	5930(39)	9992(31)	8542(34)	46(9)
C(34)	6398(34)	9277(37)	8346(34)	59(10)
N(4)	3754(36)	6000(21)	9069(20)	67(8)
O(4)	3562(23)	6023(18)	8176(14)	98(8)
O(5)	4533(14)	5633(13)	9552(13)	107(7)

2.06(4) Å (average 1.98(5) Å), and intra-C(Cp) distances from 1.49(6) to 1.33(6) Å (average 1.41(6) Å). Coordination of the Cd^{2+} ion to L^1 induces some structural changes in the ligand. The distortion appears even to affect the ferrocenyl groups. The Cp rings are planar within experimental error but are not completely parallel to each other, the angle between the planes $\text{C}(10)^i\text{--C}(14)$ and $\text{C}(10)\text{--C}(14)^i$ being 7.1° and that between the planes $\text{C}(20)\text{--C}(24)$ and $\text{C}(20)^i\text{--C}(24)^i$ being 6.4° .

Metal Coordination. Solution studies directed to the determination of the stability constants for the formation of complexes of L^1 with Pb^{2+} , Hg^{2+} , and Cd^{2+} were carried out in THF/ H_2O 70:30 (v/v ; containing 0.1 mol dm^{-3} of $(\text{Bu}_4\text{N})\text{ClO}_4$). The stability constants are given in Table 3. The behaviour of L^1 towards protonation and towards the transition-metal ions Ni^{2+} , Cu^{2+} , and Zn^{2+} has been published elsewhere [7].

All the metal ions considered here form stable $[\text{ML}^1]^{2+}$ complexes. The distribution diagram of the $\text{Hg}^{2+}/\text{L}^1/\text{H}^+$ system is depicted in Fig. 2. From pH 5 to 8 exist the species $[\text{Hg}(\text{L}^1\text{H}_2)]^{4+}$, $[\text{Hg}(\text{L}^1\text{H})]^{3+}$, and $[\text{Hg}(\text{L}^1)]^{2+}$, whereas at pH > 9 the $[\text{HgL}^1]^{2+}$ and the hydroxo species $[\text{HgL}^1(\text{OH})]^+$ coexist. The stability constants of the $[\text{CdL}^1]^{2+}$,

Table 2. Selected Bond Lengths [Å] and Angles [°] for Compound [Cd(L¹)(NO₃)₂] (1)^a

Cd(1)–N(1)	2.308(8)	Cd(1)–N(2)	2.336(11)
Cd(1)–O(1)	2.50(4)	Cd(1)–O(4)	2.50(3)
N(1)–C(1)	1.476(14)	N(1)–C(2)	1.51(2)
N(2)–C(4)	1.38(3)	N(2)–C(5)	1.39(2)
N(2)–C(3)	1.56(2)	C(1)–C(14)	1.50(2)
C(2)–C(3)	1.36(2)		
N(1) ⁱ –Cd(1)–N(1)	118.5(4)	N(1) ⁱ –Cd(1)–N(2)	162.6(4)
N(1)–Cd(1)–N(2)	78.8(4)	N(1) ⁱ –Cd(1)–N(2) ⁱ	78.8(4)
N(1)–Cd(1)–N(2) ⁱ	162.6(4)	N(2)–Cd(2)–N(2) ⁱ	83.8(6)
N(1) ⁱ –Cd(1)–O(1)	91.3(12)	N(1)–Cd(1)–O(1)	87.7(11)
N(2)–Cd(1)–O(1)	89.4(11)	N(2) ⁱ –Cd(1)–O(1)	92.1(10)
O(1)–Cd(1)–O(1) ⁱ	178(2)	N(1) ⁱ –Cd(1)–O(4)	82.5(6)
N(1)–Cd(1)–O(4)	107.4(5)	N(2)–Cd(1)–O(4)	92.6(6)
N(2) ⁱ –Cd(1)–O(4)	73.1(6)	N(1) ⁱ –Cd(1)–O(4) ⁱ	107.4(5)
N(1)–Cd(1)–O(4) ⁱ	82.5(6)	N(2)–Cd(1)–O(4) ⁱ	73.1(6)
N(2) ⁱ –Cd(1)–O(4) ⁱ	92.6(6)	O(4)–Cd(1)–O(4) ⁱ	161.1(12)

^a) i means $-x+1, y, -z+3/2$, relative to x, y, z .

Table 3. Equilibrium Data for Formation Constants (log *K*) of Cd²⁺, Pb²⁺, and Hg²⁺ Complexes with Fc₂L in THF/H₂O 70:30 (25°, 0.1 mol dm⁻³ KCl)^a

Reaction	Cd ²⁺	Pb ²⁺	Hg ²⁺
M ²⁺ + L ¹ + 2H ⁺ ↔ [M(L ¹ H ₂)] ⁴⁺	–	18.77(6)	19.50(2)
M ²⁺ + L ¹ + H ⁺ ↔ [M(L ¹ H)] ³⁺	12.46(1)	12.99(2)	13.31(1)
M ²⁺ + L ¹ ↔ [M(L ¹)] ²⁺	5.49(2)	6.08(2)	6.47(1)
M ²⁺ + L ¹ + H ₂ O ↔ [M(L ¹ (OH))] ⁺ + H ⁺	– 4.38(1)	– 2.27(2)	– 1.60(1)
[M(L ¹)] ²⁺ + H ⁺ ↔ [M(L ¹ H)] ³⁺	6.47	6.91	6.84
[M(L ¹ H)] ³⁺ + H ⁺ ↔ [M(L ¹ H ₂)] ⁴⁺	–	5.78	6.19
M ²⁺ + L ¹ + OH ⁻ ↔ [M(L ¹ (OH))] ⁺	11.27	14.05	13.38

^a) Values in parenthesis are the standard deviations in the last significant digit.

[PbL¹]²⁺, and [HgL¹]²⁺ complexes are close to those observed for Zn²⁺ [7] but are about two order of magnitude smaller than that of the corresponding [CuL¹]²⁺ complex. The stability constant for [Cu(cyclam)]²⁺ (cyclam = 1,4,8,11-tetraazacyclotetradecane) [12] in H₂O is *ca.* 10¹⁶ times larger than that of [CuL¹]²⁺. However, the stability constant of [CuL¹]²⁺ was determined in THF/H₂O 70:30, whereas that of [Cu(cyclam)]²⁺ was measured in H₂O. The stability constant of [CuL¹]²⁺ should better be compared with that of [Cu(Fc₄cyclam)]²⁺ (Fc₄cyclam = 1,4,8,11-tetrakis(ferrocenylmethyl)-1,4,8,11-tetraazacyclotetradecane) [13] which was also determined in THF/H₂O 70:30 (log *K* = 19.06). As it can be observed, the stability constant for the [CuL¹]²⁺ complex is *ca.* 10⁹ times smaller than that of the [Cu(Fc₄cyclam)]²⁺ complex in the same medium, indicating that coordination of the N-atoms to the central metal ion is less effective in L¹ than when the cyclam skeleton is considered. However, despite the larger molecular constrains in L¹, the ligand is able to act as tetradentate as it can be observed in the crystal structure of the Cd-complex **1**. Unfortunately, we were unable to grow crystals of the Hg- or Pb-complexes.

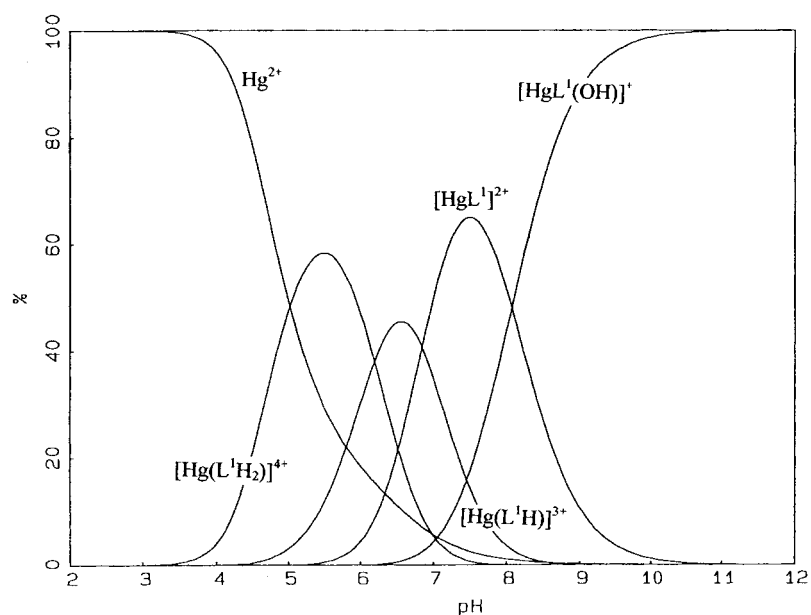


Fig. 2. Distribution diagram for the $L^1/H^+/Hg^{2+}$ system

Electrochemical Study. The oxidation potential $E_{1/2}$ of pH-responsive redox-active molecules is pH-dependent because protonation increases the molecular charge affecting the potential which has to be applied to remove an electron from the redox-active unit. This shift has been reported to be mainly electrostatic, and we have recently found that the maximum oxidation-potential shift due to the binding process with protons is a function of the number of electrons involved in the oxidation process, the number of redox units, and the distance between the redox units and the binding sites [11].

$E_{1/2}/pH$ Curves can be obtained by monitoring half-wave potential values as a function of the pH. The electrochemical behaviour of the electroactive molecule L^1 was studied using rotating disc electrode techniques. Data were obtained under the same conditions used for the potentiometric measurements (THF/H₂O 70:30 (v/v); containing 0.1 mol · dm⁻³ of (Bu₄N)ClO₄) as supporting electrolyte, Pt-electrode). We have electrochemically studied the shift of $E_{1/2}$ vs. pH for the $L^1/H^+/M^{2+}$ systems ($M = Pb^{2+}$, Hg^{2+} , or Cd^{2+} ; M^{2+}/L^1 molar ratio 1:1). A plot of the half-wave potential from rotating disc electrode experiments ($E_{1/2}$) vs. pH for the L^1/H^+ and $L^1/H^+/M^{2+}$ systems is shown in Fig. 3. The $L^1/H^+/Pb^{2+}$ and $L^1/H^+/Cd^{2+}$ curves are quite similar to that of the free ligand. However, Hg^{2+} is able to shift the oxidation potential of the ferrocenyl groups into the pH range 6–10. This suggests that there is a selective electrochemical response towards Hg^{2+} over Cd^{2+} and Pb^{2+} . In fact if the three metal ions are added to a solution of L^1 at pH 8.5, the $\Delta E_{1/2}$ ($\Delta E_{1/2} = E_{1/2}(L^1/M^{2+}) - E_{1/2}(L^1)$) observed is close to that found when only Hg^{2+} was present.

We would like to thank the DGICYT (proyecto PB95-1121-C02-02) for support.

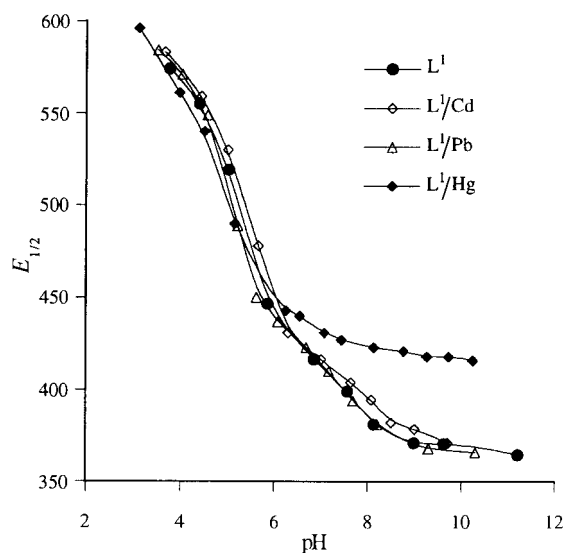


Fig. 3. $E_{1/2}$ vs. pH for the L^I/H^+ and $L^I/H^+/M^{2+}$ systems ($M^{2+} = Cd^{2+}$, Pb^{2+} , and Hg^{2+})

REFERENCES

- [1] H. Plenio, R. Diodone, *J. Organomet. Chem.* **1995**, 492, 73; H. Plenio, R. Diodene, *Inorg. Chem.* **1995**, 34, 3964.
- [2] P. D. Beer, Z. Chen, M. G. B. Drew, A. O. M. Johnson, D. K. Smith, P. Spencer, *Inorg. Chim. Acta* **1996**, 246, 143.
- [3] P. D. Beer, M. G. B. Drew, A. R. Graydon, *J. Chem. Soc., Dalton Trans.* **1996**, 4129; P. D. Beer, *J. Chem. Soc., Chem. Commun.* **1996**, 689; P. D. Beer, A. R. Graydon, A. O. M. Johnson, D. K. Smith, *Inorg. Chem.* **1997**, 36, 2112.
- [4] H. Yamamoto, A. Ori, K. Ueda, C. Dusemund, S. Shinkai, *J. Chem. Soc., Chem. Commun.* **1996**, 407.
- [5] M. E. Padilla-Tosta, R. Martínez-Máñez, T. Pardo, J. Soto, M. J. L. Tendo, *Chem. Commun.* **1997**, 887; M. J. L. Tendo, A. Benito, J. Cano, J. M. Lloris, R. Martínez-Máñez, J. Soto, A. J. Edwards, P. R. Raithby, M. A. Rennie, *J. Chem. Soc., Chem. Commun.* **1995**, 1643; M. J. L. Tendo, A. Benito, R. Martínez-Máñez, J. Soto, E. García-España, J. A. Ramírez, M. I. Burguete, S. V. Luis, *J. Chem. Soc., Dalton Trans.* **1996**, 2923; M. J. L. Tendo, A. Benito, R. Martínez-Máñez, J. Soto, *ibid.* **1996**, 4121.
- [6] J. M. Lloris, R. Martínez-Máñez, T. Pardo, J. Soto, M. E. Padilla-Tosta, *Chem. Commun.* **1998**, 837.
- [7] M. J. L. Tendo, A. Benito, R. Martínez-Máñez, J. Soto, J. Paya, A. J. Edwards, P. R. Raithby, *J. Chem. Soc., Dalton Trans.* **1996**, 343.
- [8] G. Gran, *Analyst (London)* **1952**, 77, 661. F. J. Rossotti, H. J. Rossotti, *J. Chem. Educ.* **1965**, 42, 375.
- [9] P. Gans, A. Sabatini, A. Vacca, *J. Chem. Soc., Dalton Trans.* **1985**, 1195.
- [10] 'SHELXTL, Program Version 5.03', Siemens Analytical X-Ray Instruments, Madison, WI, 1994.
- [11] A. Benito, R. Martínez-Máñez, J. Soto, M. J. L. Tendo, *J. Chem. Soc., Faraday Trans.* **1997**, 93, 2175.
- [12] M. Kodama, E. Kimura, *J. Chem. Soc., Chem. Commun.* **1975**, 891.
- [13] J. M. Lloris, R. Martínez-Máñez, T. Pardo, J. Soto, M. E. Padilla-Tosta, *J. Chem. Soc., Dalton Trans.*, in press.

Received April 29, 1998